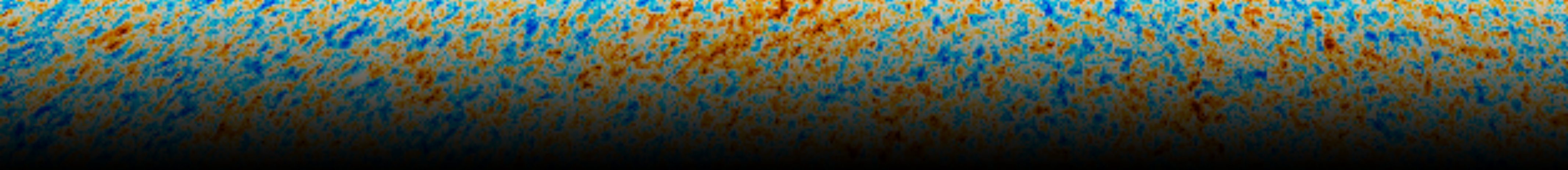

# Model-independent reconstruction of a stochastic gravitational wave background with LISA

Raphael Flauger

**Data analysis challenges for stochastic gravitational wave backgrounds**

**CERN, July 20, 2023**

# LISA

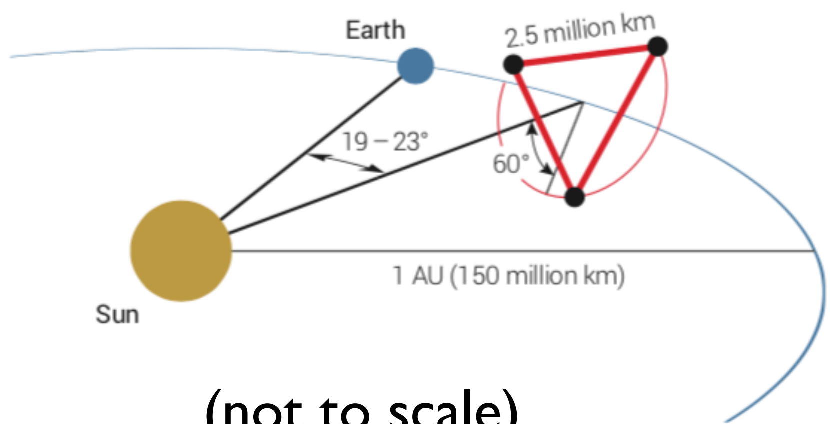


(not to scale)

arXiv:1702.00786

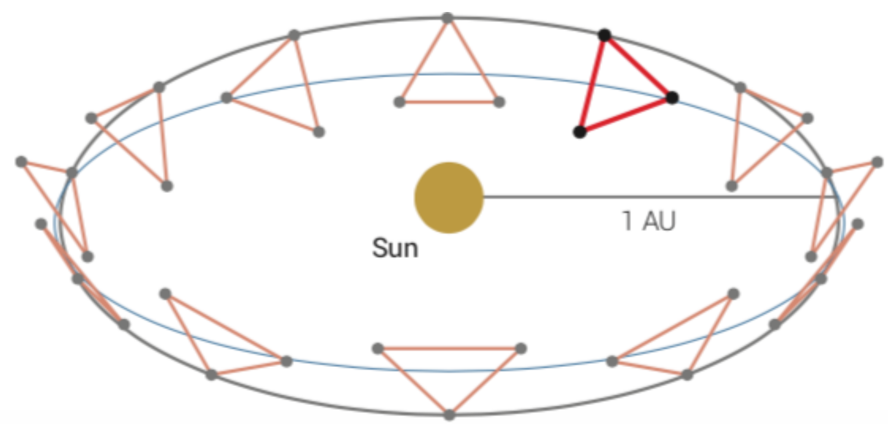


aims to detect gravitational waves with the help of time delay interferometry

# Astrophysical sources

arXiv:1702.00786

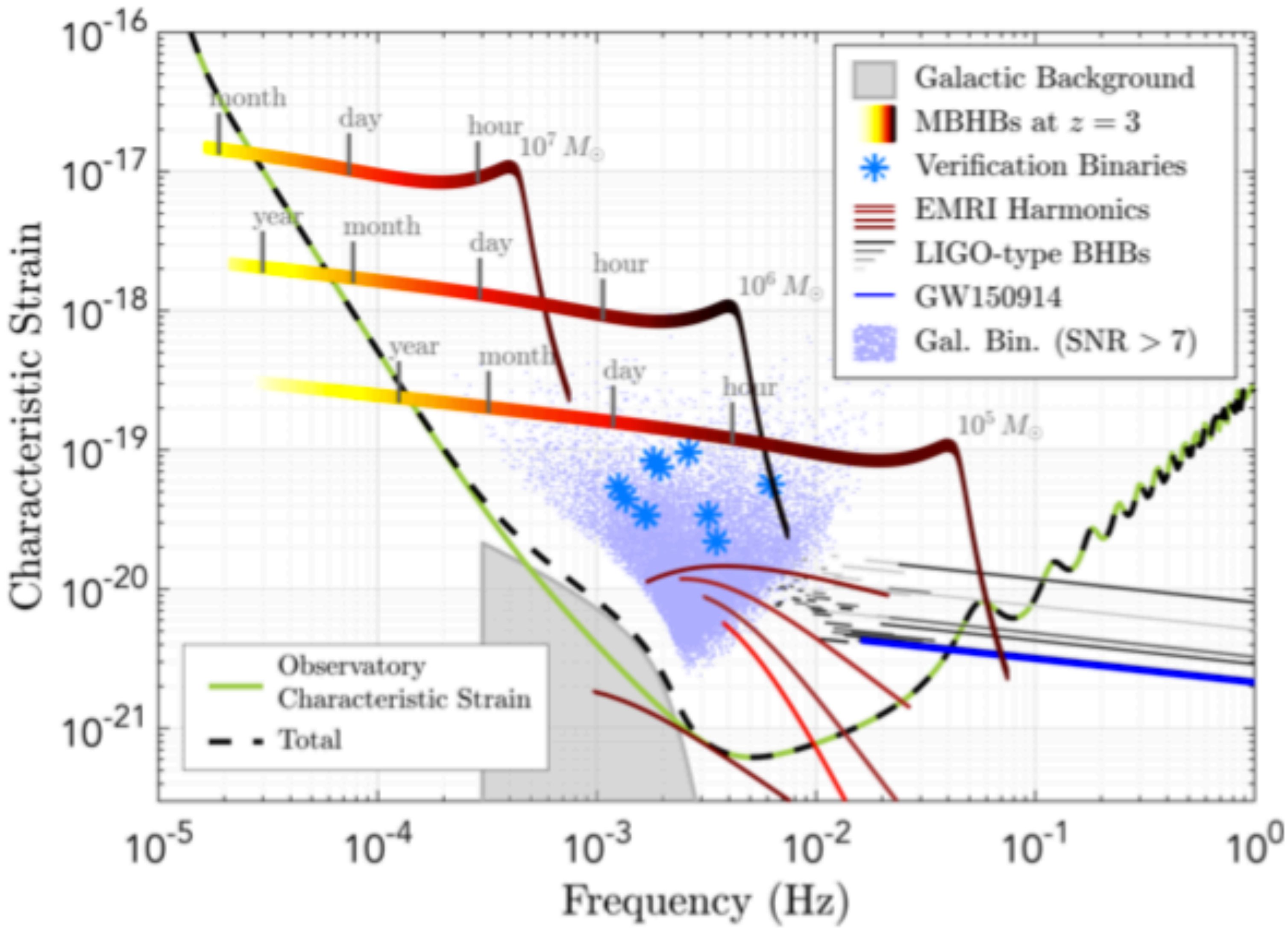

# Gravitational waves of cosmic origin

see Chiara's talk for details

# Gauge field production

Quantum fluctuations in the metric during single-field slow-roll inflation are out of LISA's reach.

If the inflaton is an axion, it is natural to expect a coupling to gauge fields that can lead to an instability in gauge field

$$\left(\frac{\partial^2}{\partial\tau^2} + k^2 \pm \frac{2k\xi}{\tau}\right) A_\pm(k,\tau) = 0 \qquad \text{with} \qquad \xi = \frac{\alpha\dot{\phi}}{2fH}$$

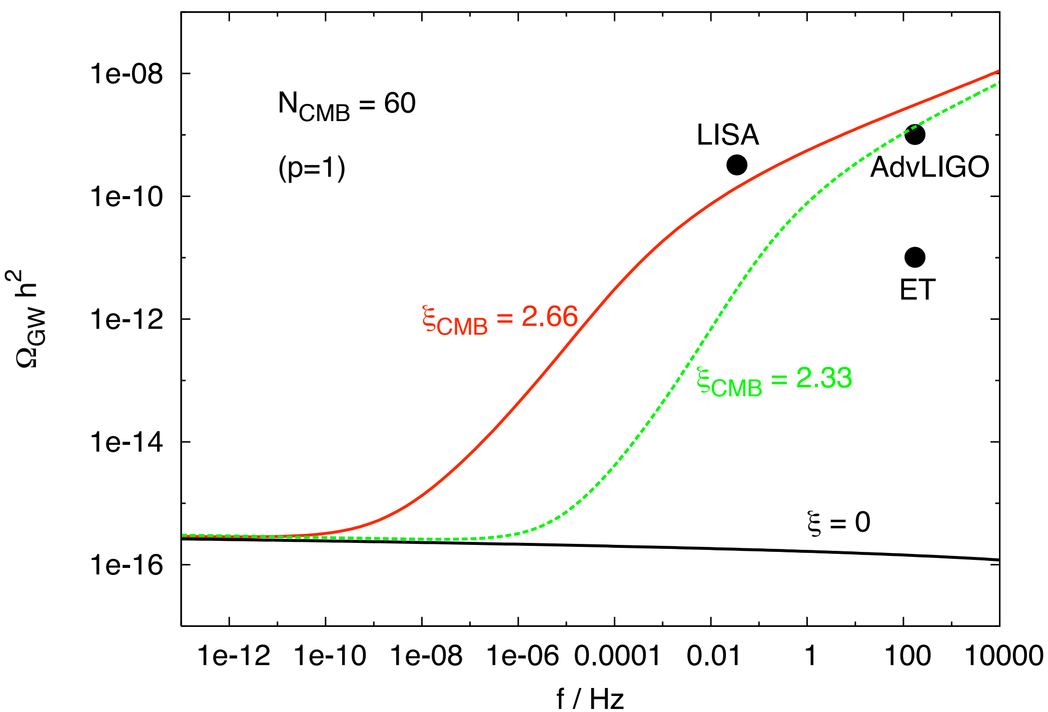


Can lead to (chiral) stochastic gravitational wave background observable with interferometers

Cook & Sorbo arXiv:1109.0022

Barnaby et al. arXiv:1110.3327

# Large Density Perturbations

On CMB scales, the primordial power spectrum of density perturbations is small and tightly constrained.

For the simplest models of inflation, the power spectrum is nearly scale invariant, but the perturbations could be significantly larger on small scales because of

- a decrease in inflaton speed
- a change in sound speed
- a sharp turn in field space
- …

# Large Density Perturbations

Density perturbations generate gravitational waves at second order. Upper limits on stochastic gravitational wave background constrain features in spectrum of primordial density perturbations.

Primordial black holes formed at horizon reentry contribute to the stochastic gravitational wave background through mergers and close encounters.

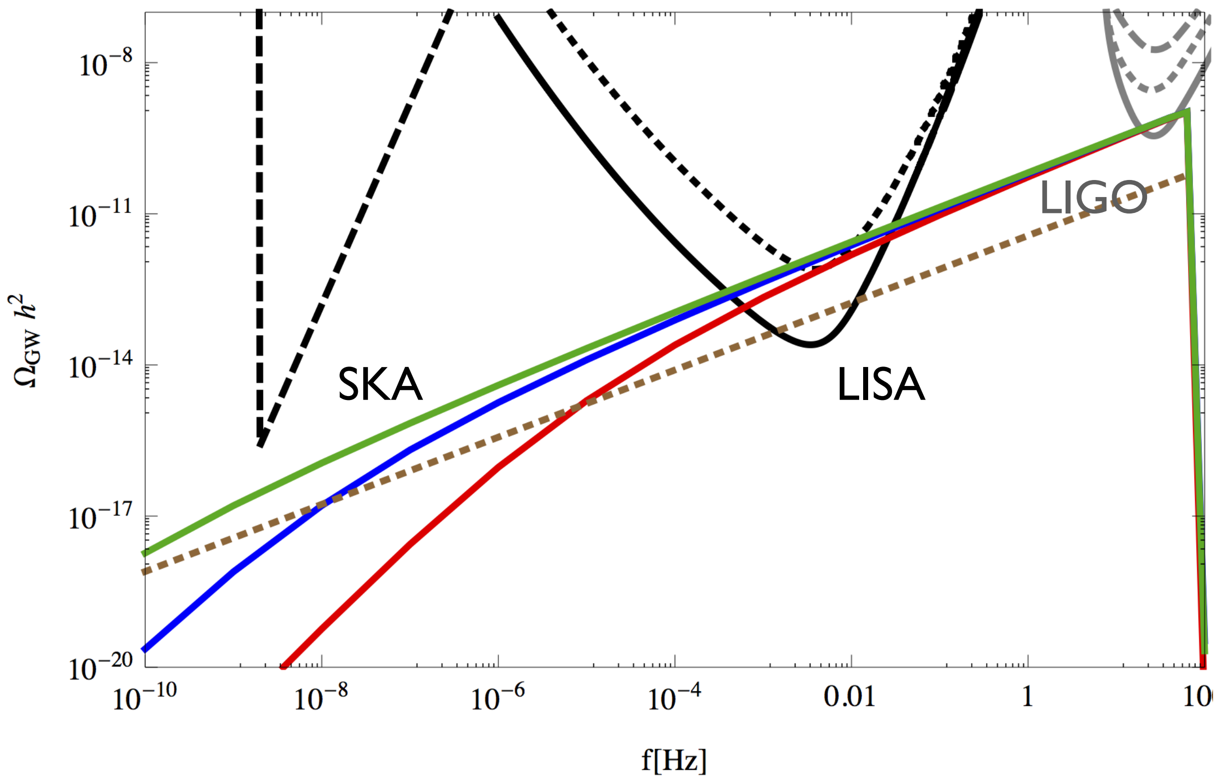


Clesse, García-Bellido arXiv:1610.08479

# First order phase transitions

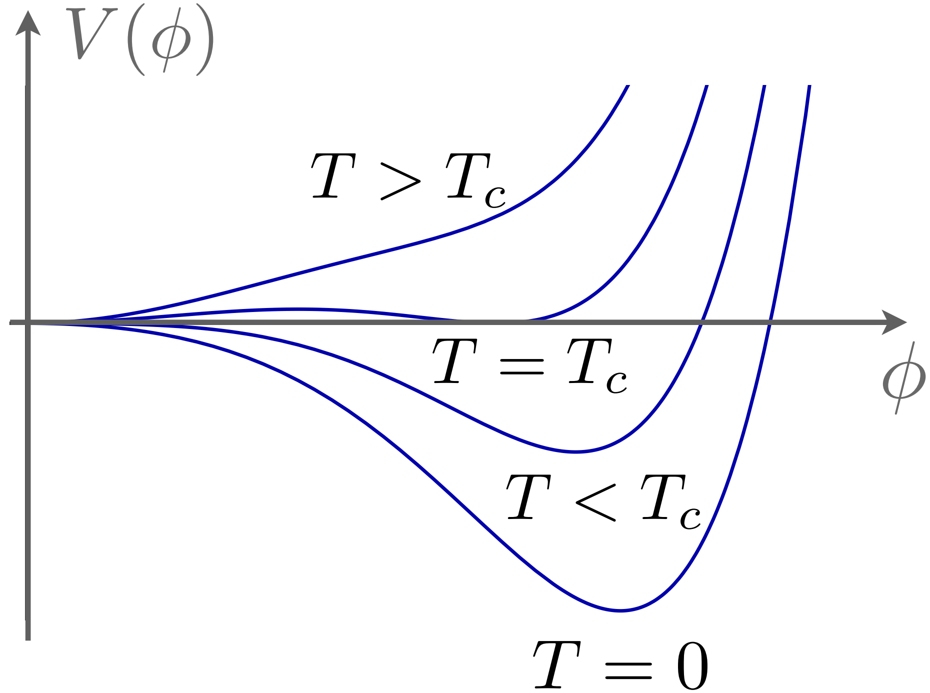


The phase transition proceeds via nucleation of bubbles of the true vacuum.

# First order phase transitions

Gravitational wave sources

Bubble collisions and subsequent scalar field dynamics

$$T_{ij} \supset \partial_i \phi \partial_j \phi$$

If the transition occurs in a medium, sound waves are created as the bubbles expand

$$T_{ij} \supset \gamma^2 (p + \rho) v_i v_j$$

MHD turbulence (in the presence of electromagnetic fields)

$$T_{ij} \supset E_i E_j + B_i B_j - \frac{1}{3} \delta_{ij} (E^2 + B^2)$$

# First order phase transitions

The peak frequency is set by the scale of the phase transition, and LISA can constrain first order phase transitions around the electroweak scale.

(adapted from) Caprini et al. arXiv:1512.06239

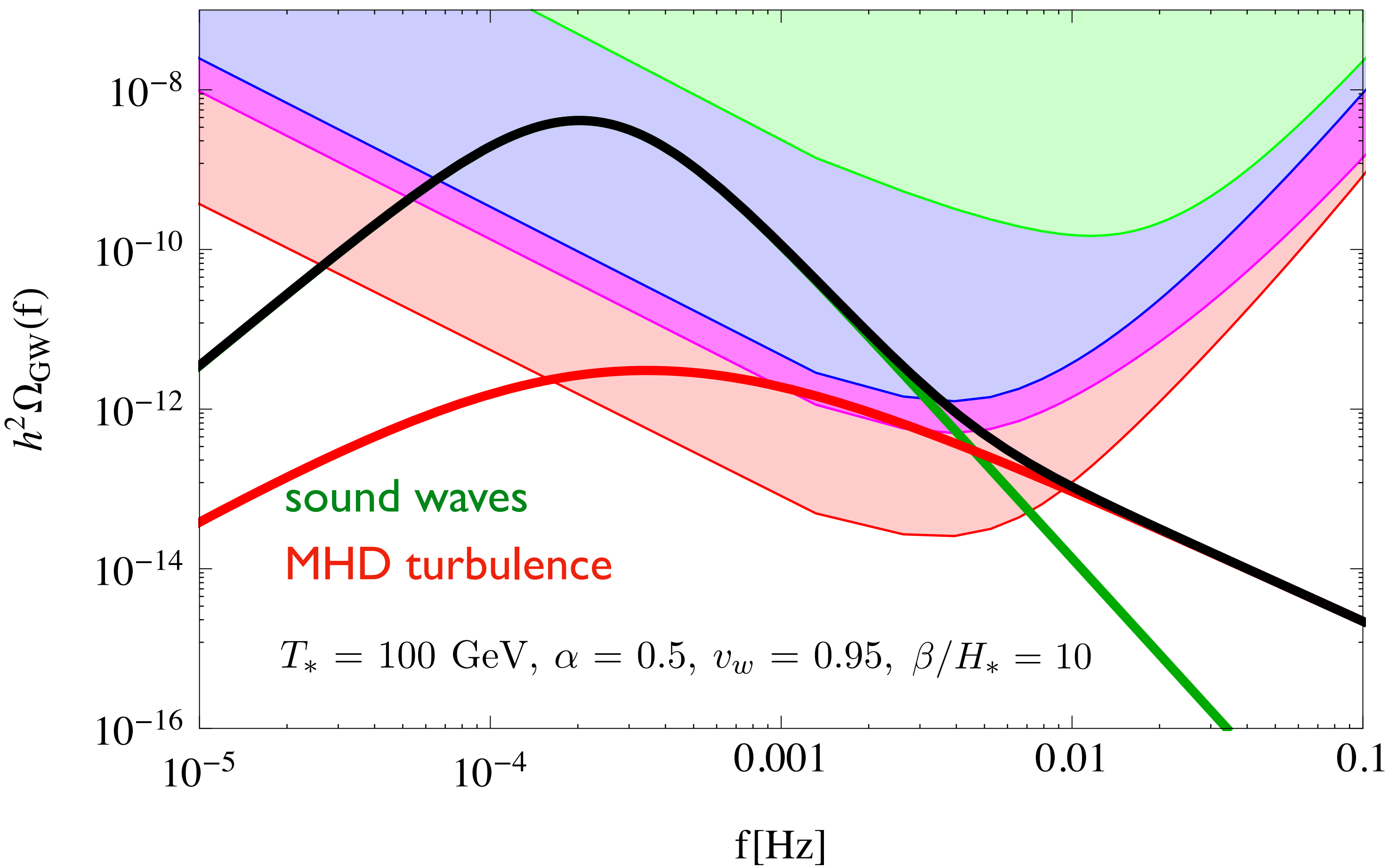

# Topological defects

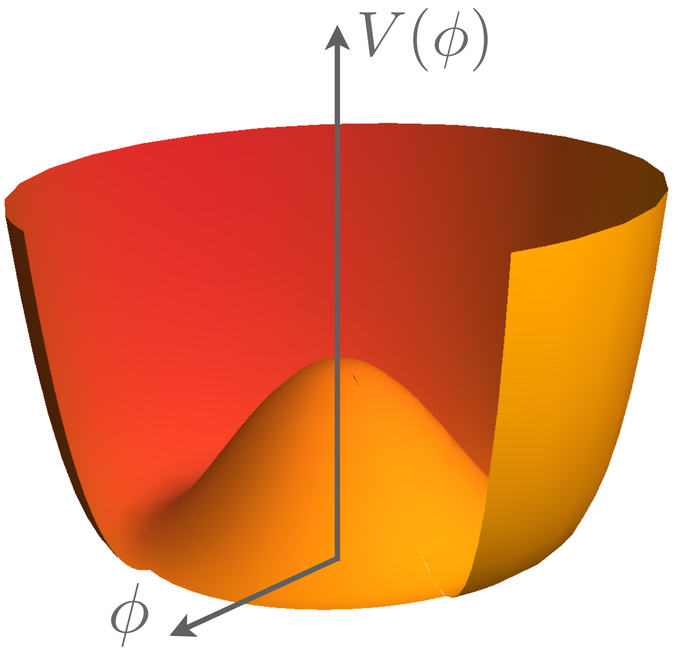


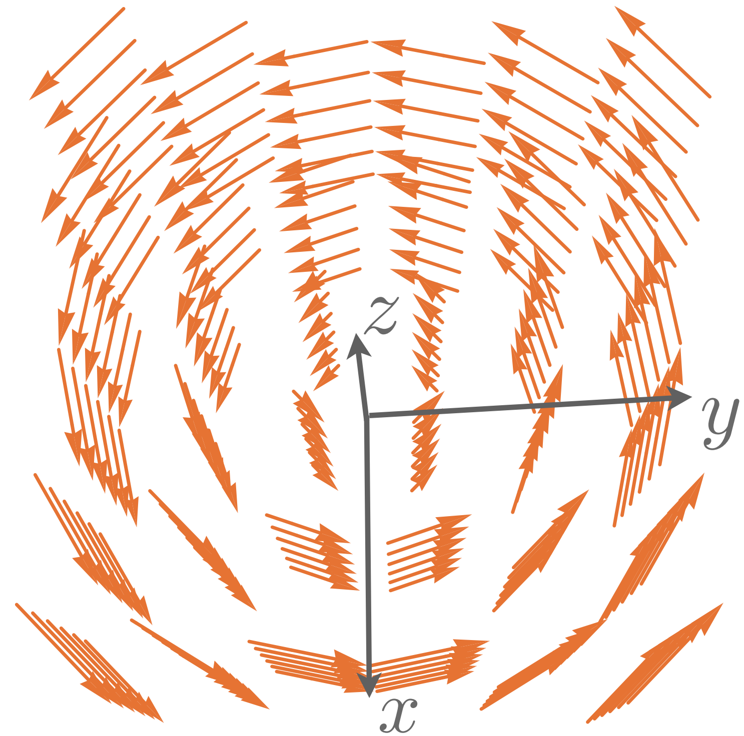


Phase transitions that involve spontaneous symmetry breaking often lead to defects.

# Cosmic Strings

After the phase transition we are left with a network of strings

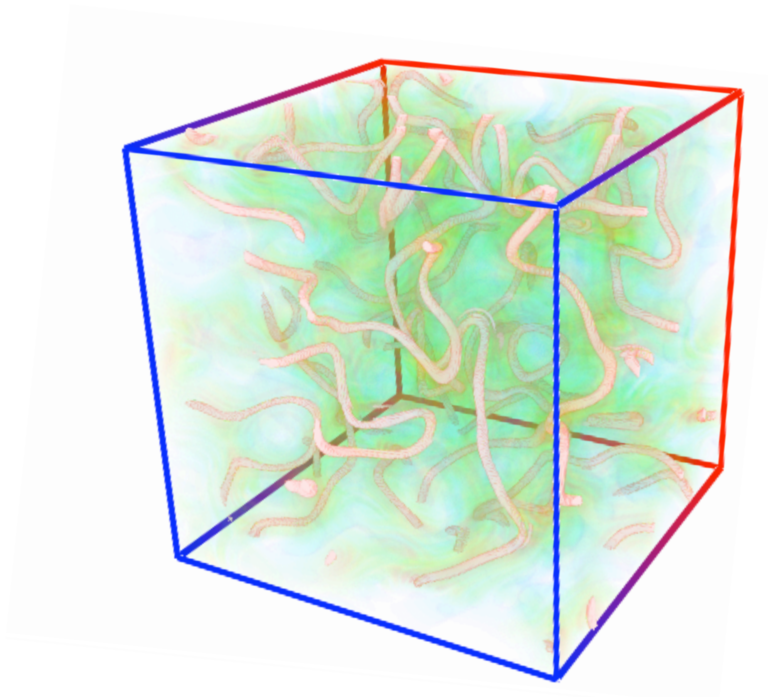

Dufaux et al.
arXiv:1006.0217

In the absence of interactions these strings would rapidly begin to dominate the energy density as

$$\rho_\infty \propto a^{-2}$$

$$\rho_\circ \propto a^{-3}$$

# Cosmic Strings

Loops form when strings inter- or  autocommute

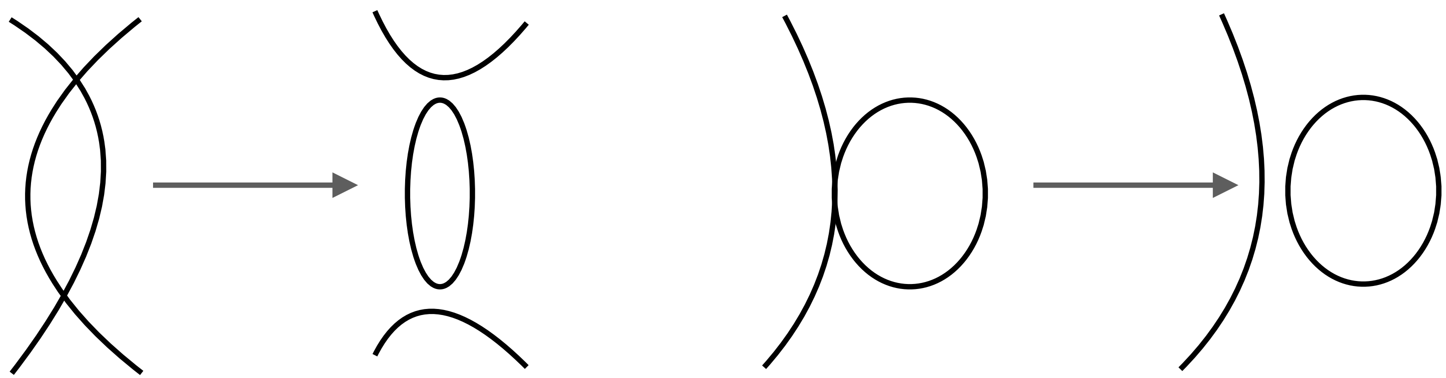

These can decay into smaller loops through self-intersection.

These processes lead to a scaling solution

$$\rho_s = \frac{\mu L}{L^3} = \frac{\mu}{L^2} \propto \mu H^2 \qquad \text{so} \qquad \frac{\rho_s}{\rho_r} = \text{const}$$

# Cosmic Strings

Gravitational wave spectrum

adapted from Auclair et al. arXiv:1909.00819

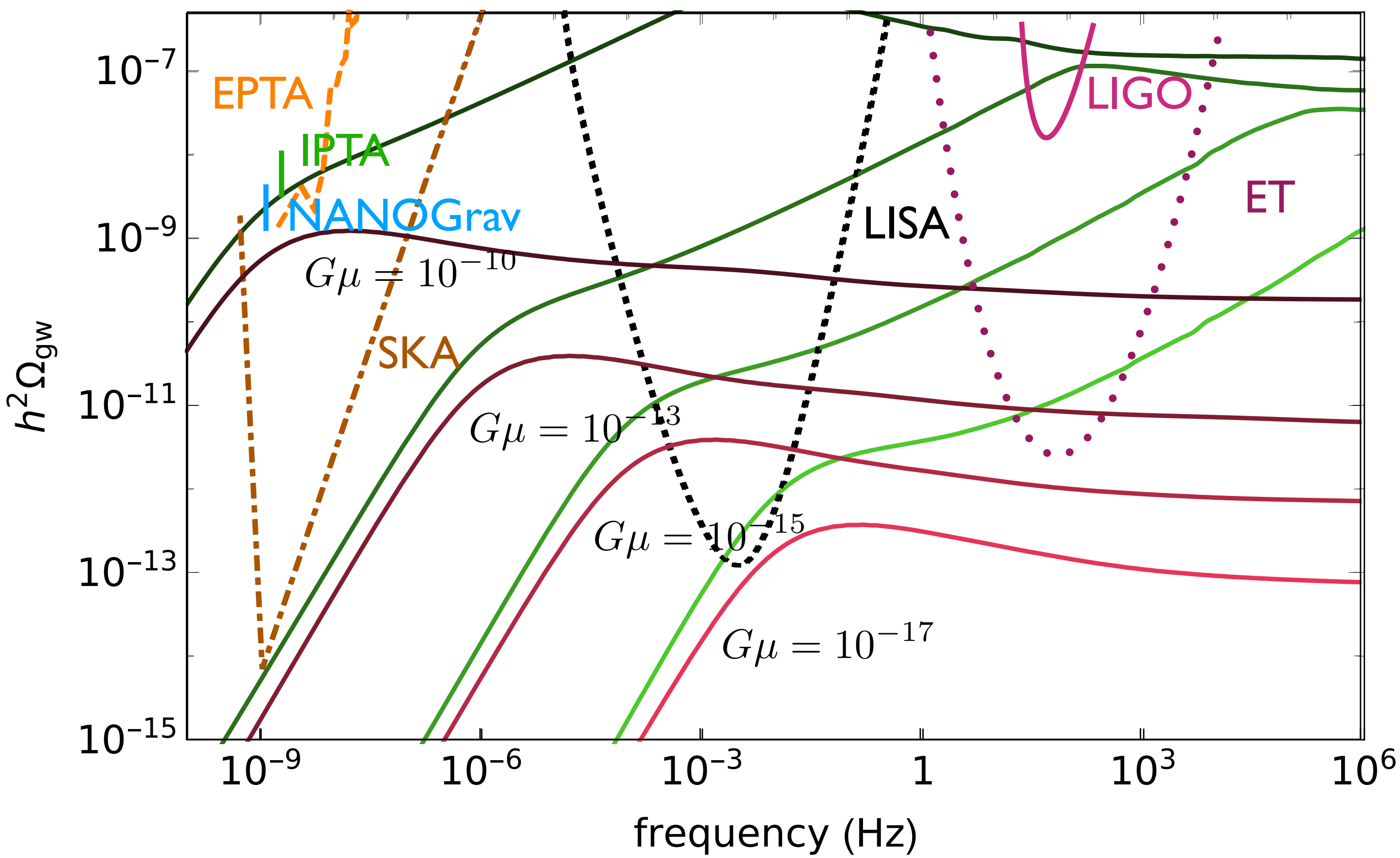

# Model-independent constraints

Two preliminary take-aways

There are several potential sources of cosmological gravitational wave backgrounds LISA can constrain and could detect. The fact that the spectra vary widely between models motivates a model-independent search.

To constrain stochastic gravitational wave backgrounds, we constrain any excess over noise. So we must understand/measure the noise properties to do this successfully.

# Time delay interferometry

# Time delay interferometry

Neglecting the effect of gravitational potentials and treating the satellites as free-falling in a background of gravitational waves in Minkowski space, we can write the line element as

$$ds^2 = -dt^2 + (\delta_{ij} + h_{ij}(\mathbf{x}, t))dx^i dx^j$$

Free-falling massive particles whose initial comoving momenta vanish remain at fixed comoving position

$$X^i(t) = x_a^i$$

So their physical distance varies as gravitational waves pass by

# Time delay interferometry

Photons transmitted from one free-falling satellite to another then acquire a time delay. To leading order in the strain, for photons arriving at $b$ at time $t$ the time delay is

$$\Delta T_{ba}(t) = \frac{1}{2}\hat{n}_{ba}^i \hat{n}_{ba}^j \int_0^{L_{ba}} ds\, h_{ij}(\mathbf{x}_a + \hat{n}_{ba} s, t - L_{ba} + s)$$

unit vector from $a \to b$

unperturbed distance

We can hope to measure these time delays, or equivalently the associated frequency shifts with help of interferometry.

# Time delay interferometry

Considering the drift in the central frequency of the laser as the only source of uncertainty, the measured Doppler shift is

$$\Delta_{ba}(t) = s_{ba}(t) + p_a(t - L_{ba}) - p_b(t)$$

where $s$ is the relative change in frequency and $p_a(t)$ is the laser frequency noise of the laser at satellite $a$ at time $t$.

Since the $p_a(t)$ are much larger than the signal (and other sources of noise), we must form linear combinations in which they cancel.

# Time delay interferometry

As a simple example, we can consider a Michelson interferometer

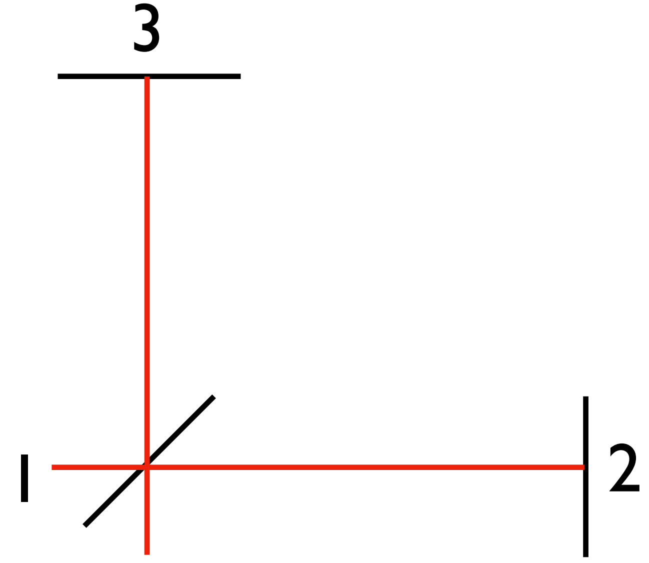


where we can define

$$
\begin{aligned}
M_1(t) &= \Delta_{21}(t - L_{12}) + \Delta_{12}(t) - \Delta_{31}(t - L_{13}) - \Delta_{13}(t) \\
&= s_{21}(t - L_{12}) + s_{12}(t) - s_{31}(t - L_{13}) - s_{13}(t) \\
&\qquad + p_1(t - 2L_{12}) - p_1(t - 2L_{13})
\end{aligned}
$$

# Time delay interferometry

If the arm lengths are equal,

$$L_{12} = L_{13} = L$$

the laser frequency noise cancels

$$M_1(t) = s_{21}(t - L) + s_{12}(t) - s_{31}(t - L) - s_{13}(t)$$

For unequal armlengths we have to define more complicated variables to cancel laser frequency noise.

# Time delay interferometry

One such variable is

$$\begin{aligned} X(t) = & \ \underline{\Delta_{21}(t - L_{12} - 2L_{13}) + \Delta_{12}(t - 2L_{13}) + \Delta_{31}(t - L_{13}) + \Delta_{13}(t)} \\ & - \underline{\Delta_{31}(t - L_{13} - 2L_{12}) - \Delta_{13}(t - 2L_{12}) - \Delta_{21}(t - L_{12}) - \Delta_{12}(t)} \\ = & \ s_{21}(t - L_{12} - 2L_{13}) + s_{12}(t - 2L_{13}) + s_{31}(t - L_{13}) + s_{13}(t) \\ & - s_{31}(t - L_{13} - 2L_{12}) - s_{13}(t - 2L_{12}) - s_{21}(t - L_{12}) - s_{12}(t) \end{aligned}$$

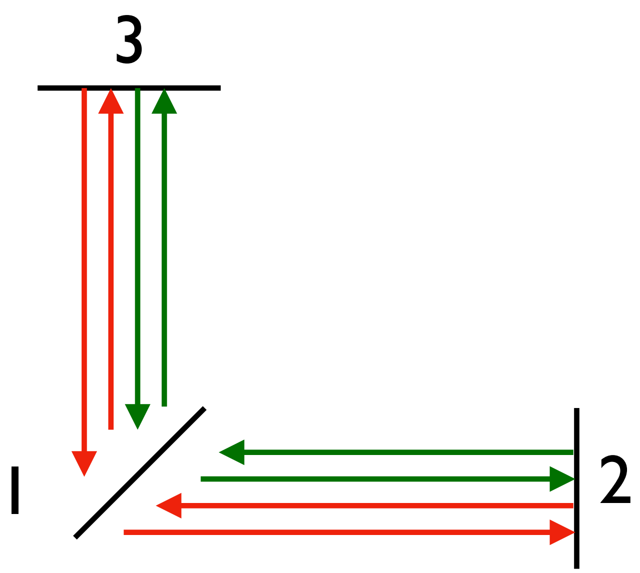


By cyclic permutation, one obtains the variables Y and Z.

# Time delay interferometry

For a triangular configuration, we can also consider

$$\begin{aligned}\alpha(t) = \;& \underline{\Delta_{21}(t - L_{13} - L_{23}) + \Delta_{32}(t - L_{13}) + \Delta_{13}(t)} \\ & - \underline{\Delta_{31}(t - L_{12} - L_{23}) - \Delta_{23}(t - L_{12}) - \Delta_{12}(t)} \\ = \;& s_{21}(t - L_{13} - L_{23}) + s_{32}(t - L_{13}) + s_{13}(t) \\ & - s_{31}(t - L_{12} - L_{23}) - s_{23}(t - L_{12}) - s_{12}(t)\end{aligned}$$

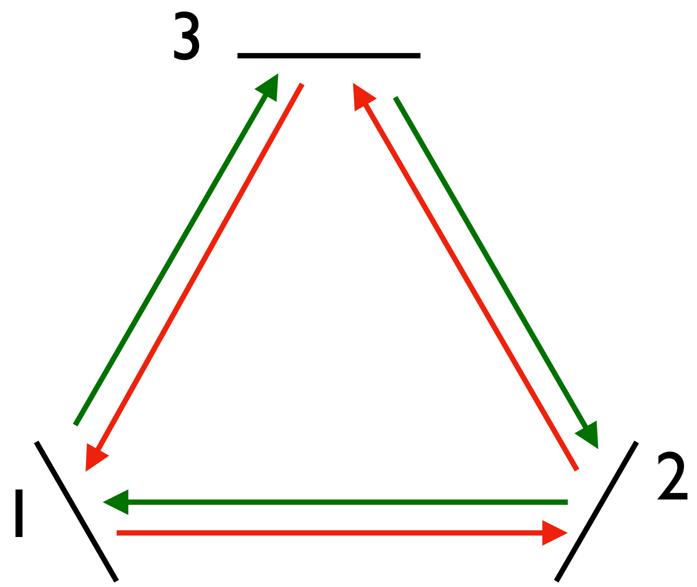


corresponding to a Sagnac interferometer

# Time delay interferometry

To understand TDI variables systematically, one might ask what mathematical problem they are a solution to.

Introducing the translation operators

$$D_{ij} f(t) = f(t - L_{ij})$$

The Doppler variables become

$$\Delta_{ba}(t) = s_{ba}(t) + D_{ba} p_a(t) - p_b(t)$$

and, e.g., the Sagnac variable becomes

$$\alpha = D_{13} D_{23} \Delta_{21} + D_{13} \Delta_{32} + \Delta_{13} - D_{12} D_{23} \Delta_{31} - D_{12} \Delta_{23} - \Delta_{12}$$

# Time delay interferometry

Good TDI variables are then variables

$$\sum_{\substack{a,b \\ a \neq b}} q_{ba} \Delta_{ba}$$

such that

$$\sum_{\substack{a,b \\ a \neq b}} q_{ba} (D_{ba} p_a - p_b) = 0$$

where the q's are polynomials in the translation operators

Since this must hold for arbitrary p, these are conditions on the polynomials and is a problem in commutative algebra. The space of solutions can be characterized by an exact sequence.

See Mauro’s talk for more details on TDI variables.

# Time delay interferometry

So far we have focused exclusively on laser frequency noise, but there are other sources of noise, including photon shot noise and acceleration noise.

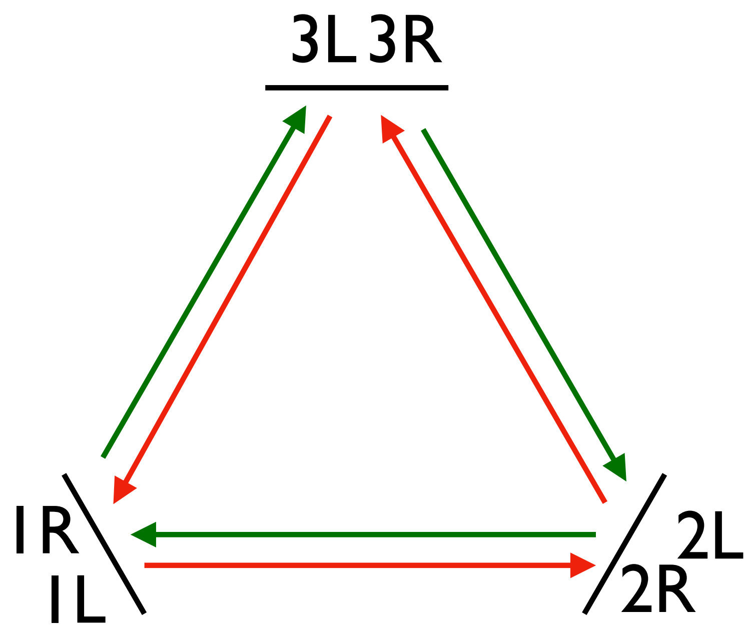


shot noise

$$\Delta_{12} = D_{12} p_{2R} - p_{1L} + \hat{n}_{12}(D_{12}\mathbf{V}_{2R} + \mathbf{V}_{1L} - 2\mathbf{v}_{1L}) + n_{12}$$

velocity fluctuations of optical benches

velocity fluctuations of probe masses

# Time delay interferometry

So far we have focused exclusively on laser frequency noise, but there are other sources of noise, including photon shot noise and acceleration noise.

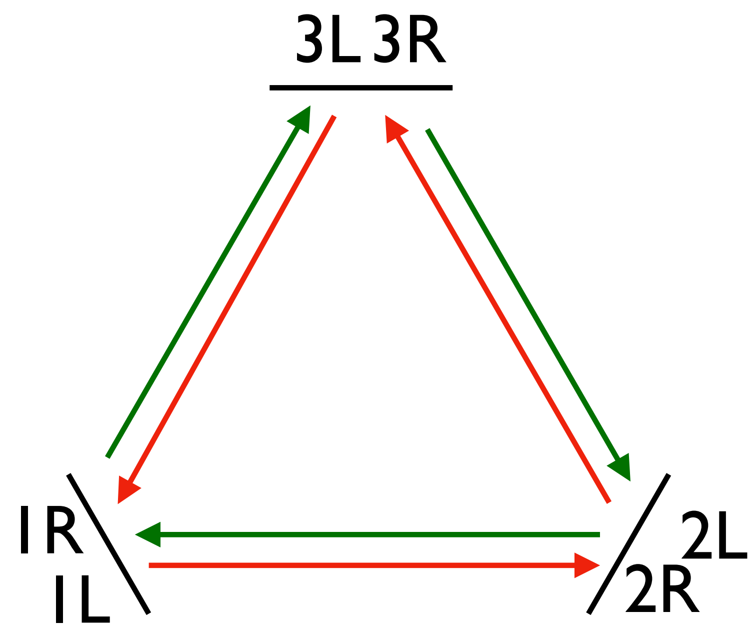


$$\Delta_{12} = D_{12}\phi_{2R} - \phi_{1L} - 2\hat{n}_{12}\cdot\mathbf{v}_{1L} + n_{12}$$

shot noise

cancel in TDI variables

leads to acceleration noise

# Time delay interferometry

In Fourier space the translation operators are diagonal and simply become

$$D_{ab} \to e^{2\pi i f L_{ab}}$$

Then, for example, for the Sagnac variable

$$\alpha = D_{13}D_{23}\Delta_{21} + D_{13}\Delta_{32} + \Delta_{13} - D_{12}D_{23}\Delta_{31} - D_{12}\Delta_{23} - \Delta_{12}$$

the shot noise contribution in Fourier space becomes

$$\begin{aligned}\tilde{\alpha} =& e^{2\pi i f(L_{13}+L_{23})}\tilde{n}_{21} + e^{2\pi i f L_{13}}\tilde{n}_{32} + \tilde{n}_{13} \\ & - e^{2\pi i f(L_{12}+L_{23})}\tilde{n}_{31} - e^{2\pi i f L_{12}}\tilde{n}_{23} - \tilde{n}_{12}\end{aligned}$$

# Time delay interferometry

Assuming that the different links are uncorrelated and statistically identical

$$\langle \tilde{n}_{12}(f)\tilde{n}_{12}(f')\rangle' = \langle \tilde{n}_{23}(f)\tilde{n}_{23}(f')\rangle' = \cdots = P_{\rm IMS}(f)$$

the contribution the noise auto-power spectrum is then

$$\langle \tilde{\alpha}(f)\tilde{\alpha}^*(f')\rangle' = 6P_{\rm IMS}(f)$$

Similarly for the X, Y, Z variables

$$\begin{aligned}\langle X(f)X^*(f')\rangle' &= 8\left(\sin^2\left(2\pi f L_{12}\right) + \sin^2\left(2\pi f L_{13}\right)\right) P_{\rm IMS}(f) \\ \langle X(f)Y^*(f')\rangle' &= -8e^{2\pi i f(L_{13}-L_{23})}\sin\left(2\pi f L_{13}\right)\sin\left(2\pi f L_{23}\right) \\ &\qquad \times \cos\left(2\pi f L_{12}\right) P_{\rm IMS}(f)\end{aligned}$$

with the remaining spectra related by cyclic permutation.

# Time delay interferometry

Similarly, assuming that the velocity perturbations of the test masses are uncorrelated and statistically identical

$$\langle \hat{n}_{12}\tilde{\mathbf{v}}_{1L}(f)\hat{n}_{12}\tilde{\mathbf{v}}^*_{1L}(f')\rangle' = \langle \hat{n}_{13}\tilde{\mathbf{v}}_{1R}(f)\hat{n}_{13}\tilde{\mathbf{v}}^*_{1R}(f')\rangle' = \cdots = P_{\rm acc}(f)$$

the acceleration noise contributes

$$\begin{aligned}\langle X(f)X^*(f')\rangle' = 8\big(&2\sin^2(2\pi f L_{12}) + 2\sin^2(2\pi f L_{13}) \\ &+ \sin^2(2\pi f(L_{12}-L_{13})) + \sin^2(2\pi f(L_{12}+L_{13}))\big)P_{\rm acc}(f) \\ \langle X(f)Y^*(f')\rangle' = -&32 e^{2\pi i f(L_{13}-L_{23})}\sin(2\pi f L_{13})\sin(2\pi f L_{23})\cos(2\pi f L_{12})P_{\rm acc}(f)\end{aligned}$$

with the remaining spectra related by cyclic permutation.

# SGWBinner

w/
Chiara Caprini, Dani Figueroa, Nikolaos Karnesis, Germano Nardini, Marco Peloso, Mauro Pieroni, Angelo Ricciardone, Gianmassimo Tassinato, Jesús Torrado

# LISA noise model

In the X, Y, Z basis and assuming an equilateral configuration, the noise spectra are

$$N_{aa}(f,A,P) = 16\sin^2\left(\frac{2\pi f L}{c}\right)\left\{\left[3+\cos\left(\frac{4\pi f L}{c}\right)\right]P_{\mathrm{acc}}(f,A) \right.$$
$$\left. + P_{\mathrm{IMS}}(f,P)\right\}$$

$$N_{ab}(f,A,P) = -8\sin^2\left(\frac{2\pi f L}{c}\right)\cos\left(\frac{2\pi f L}{c}\right)$$
$$\times\left[4P_{\mathrm{acc}}(f,A) + P_{\mathrm{IMS}}(f,P)\right]$$

Diagonalization leads to the A, E, T basis.

# LISA noise model

To fully characterize the spectra, we need the IMS and acceleration noise spectra. We assume some information will be available and in practice used

$$P_{\rm IMS}(f,P) = P^2\ \frac{\rm pm^2}{\rm Hz}\left[1+\left(\frac{2\,\rm mHz}{f}\right)^4\right]\left(\frac{2\pi f}{c}\right)^2$$

$$P_{\rm acc}(f,A) = A^2\ \frac{\rm fm^2}{\rm s^4\,Hz}\left[1+\left(\frac{0.4\,\rm mHz}{f}\right)^2\right] \times\left[1+\left(\frac{f}{8\,\rm mHz}\right)^4\right]\left(\frac{1}{2\pi f}\right)^4\left(\frac{2\pi f}{c}\right)^2$$

# LISA noise model

We see that the IMS and acceleration noise spectra are necessary to specify the noise covariance matrix. We assume some information will be available and in practice, we used

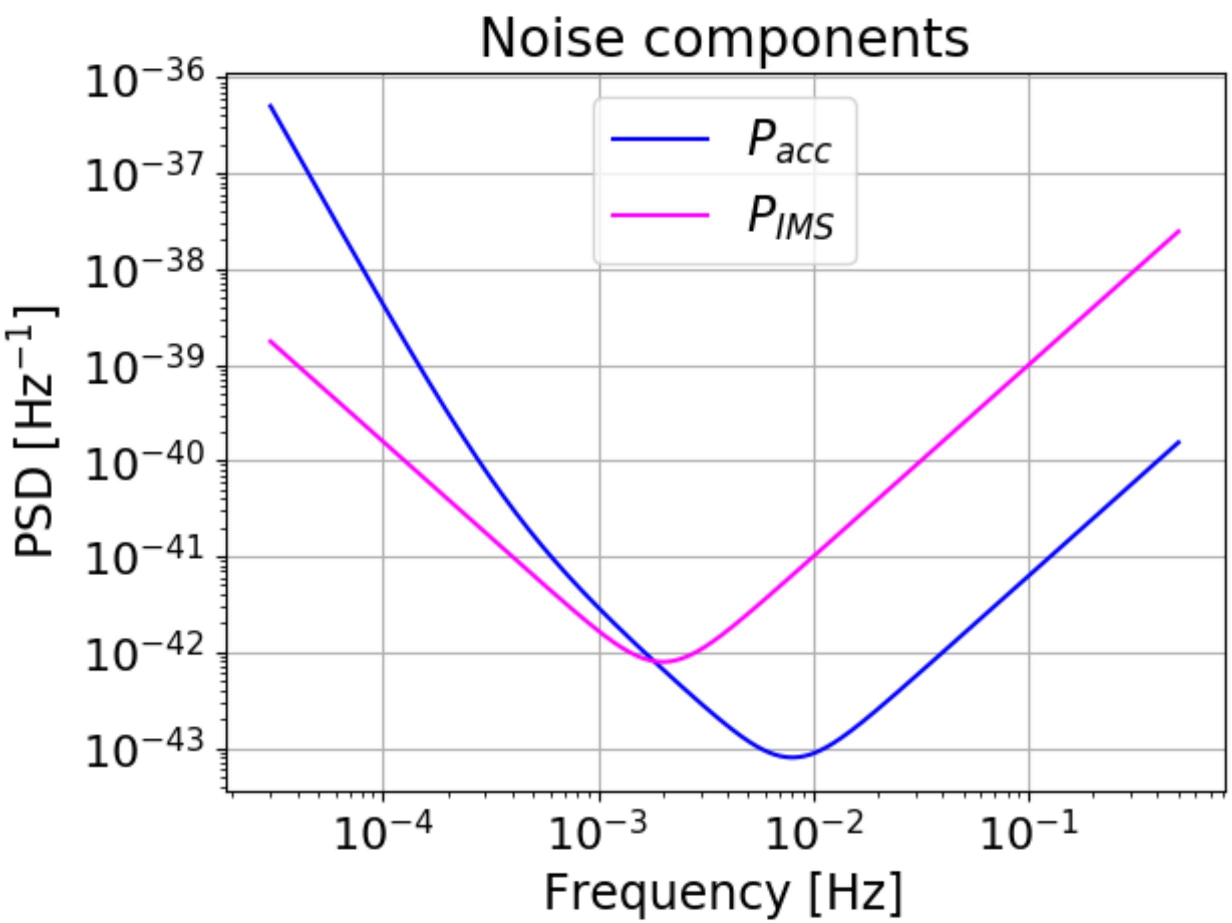

# LISA noise model

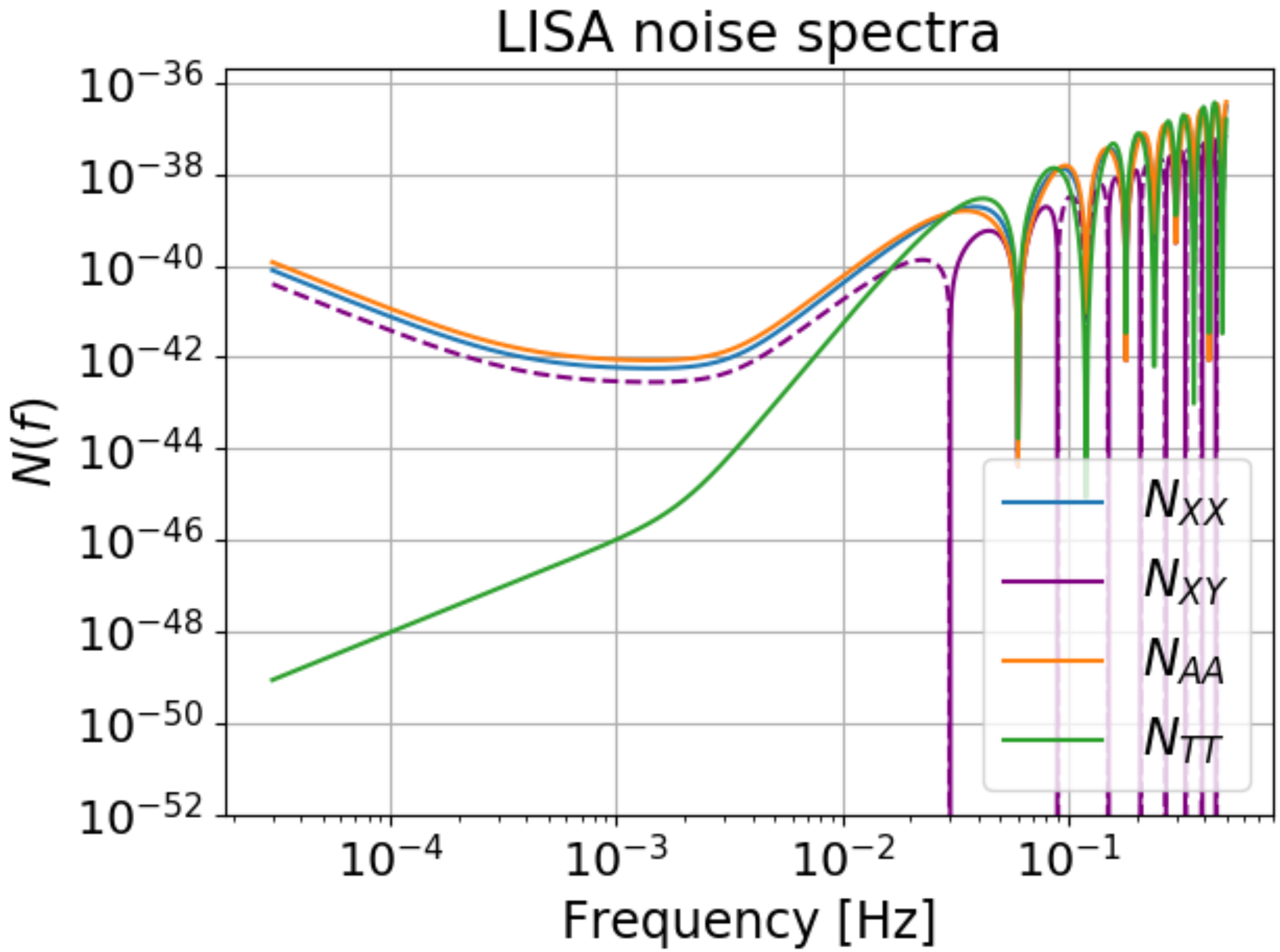

# Likelihood

For concreteness, consider some model with parameters $\theta$.

Given the data $D$, we would like to know which choice of parameters provides the best fit.

Using Bayes' theorem

Prior

$$P(\theta|D) \propto \mathcal{L}(\theta)P(\theta)$$

Likelihood

# Likelihood

In general, the parameters include both cosmological parameters and noise parameters.

We impose Gaussian priors on the parameters of the noise model and work with uniform priors on cosmological parameters

$$P(\theta, n|D) \propto \mathcal{L}(\theta, n)P(n)$$

The parameters could be the values of the power spectrum in different bins, or could be parameters of the underlying model.

# Likelihood

If a given data point is based on a large number of underlying measurements, we expect the likelihood to be Gaussian

$$\ln \mathcal{L}_G(D|\vec{\theta},\vec{n}) = -\frac{N_{\rm c}}{2}\sum_{i,j}\sum_{k} n_{ij}^{(k)} \left[\frac{\mathcal{D}_{ij}^{th}(f_{ij}^{(k)},\vec{\theta},\vec{n}) - \mathcal{D}_{ij}^{(k)}}{\mathcal{D}_{ij}^{th}(f_{ij}^{(k)},\vec{\theta},\vec{n})}\right]^2$$

channels

bins

where

$$\mathcal{D}_{ij}^{th}(f,\vec{\theta},\vec{n}) \equiv \mathcal{R}_{ij}\Omega_{GW}h^2(f,\vec{\theta}) + \Omega_{n,ij}h^2(f,\vec{n})$$

# Likelihood

In practice for our choices non-Gaussianity is not yet completely negligible and we correct the likelihood

$$\ln \mathcal{L} = \frac{1}{3} \ln \mathcal{L}_G + \frac{2}{3} \ln \mathcal{L}_{LN}$$

where

$$\ln \mathcal{L}_{LN}(D|\vec{\theta}, \vec{n}) = -\frac{N_{\rm c}}{2} \sum_{i,j} \sum_k n_{ij}^{(k)} \ln^2 \left[ \frac{\mathcal{D}_{ij}^{th}(f_{ij}^{(k)}, \vec{\theta}, \vec{n})}{\mathcal{D}_{ij}^{(k)}} \right]$$

This can then be used to search for any model for which the dependence of the signal on some set of $\theta$ is known. Some likelihood characterizing the data after a global fit for resolved sources should be an official data product.

# SGWBinner

- Obtain prior on noise parameters from TT channel
- Bin signal to initial (and maximal) number of bins
- Find best-fit parameters for each bin for signal (taken as power law) and noise parameters (subject to prior)
- Check whether merging neighboring bins is statistically preferred (according to AIC) and merge if necessary
- Repeat fitting for signal and noise parameters if merge was performed
- Once bins have converged, estimate error locally or globally with MCMC.

# Examples

Power law

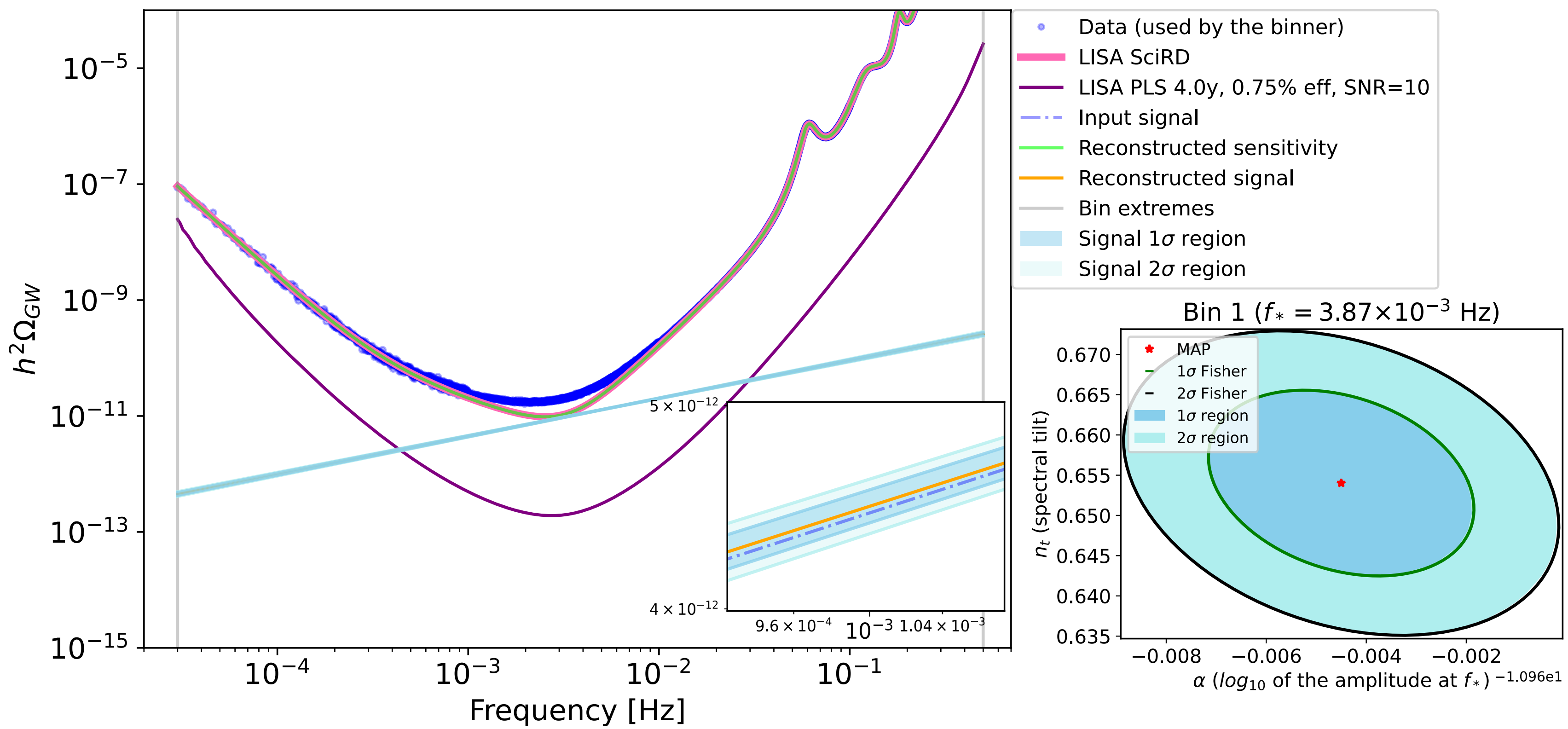

# Examples

## Broken power law

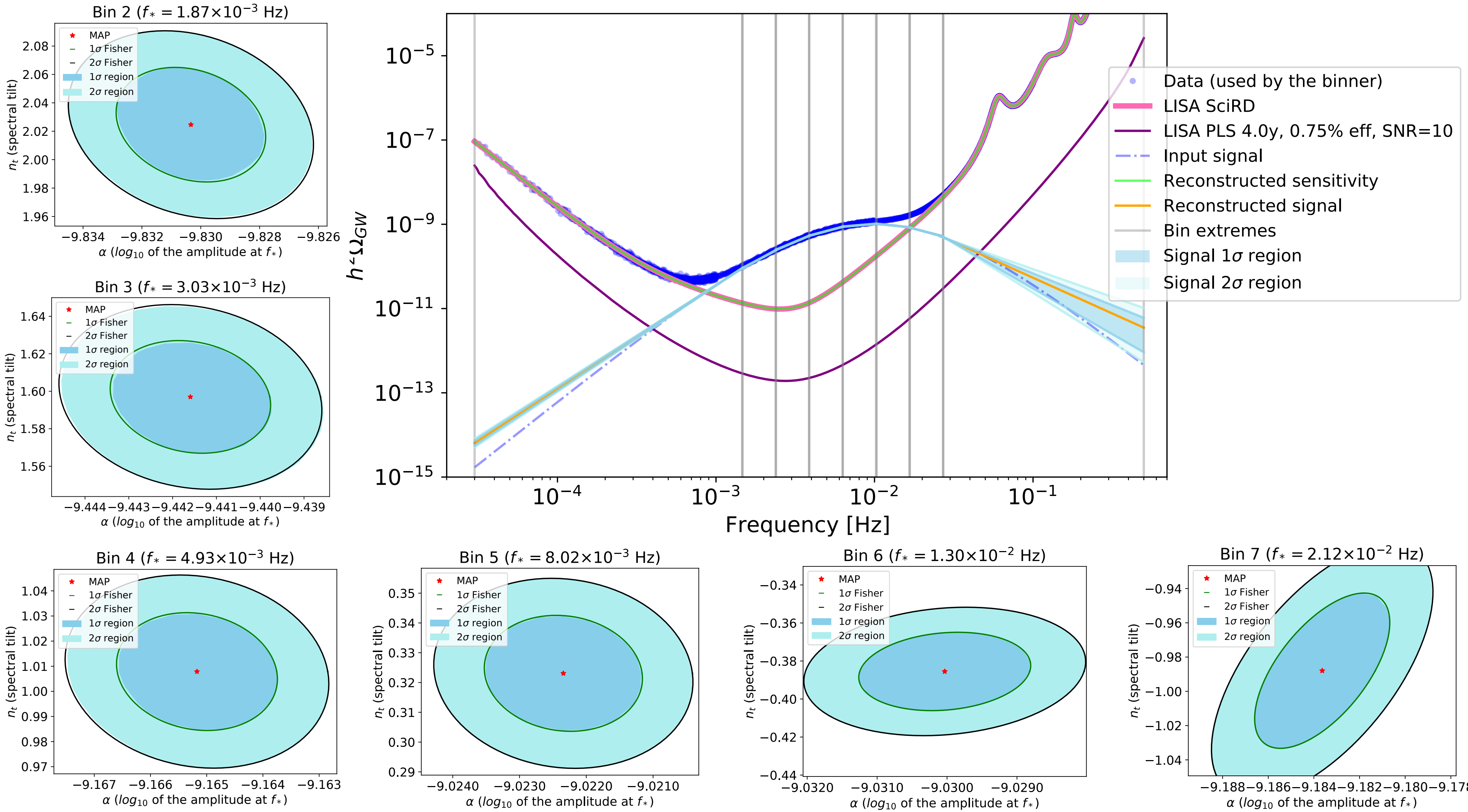

# Examples

## Bump

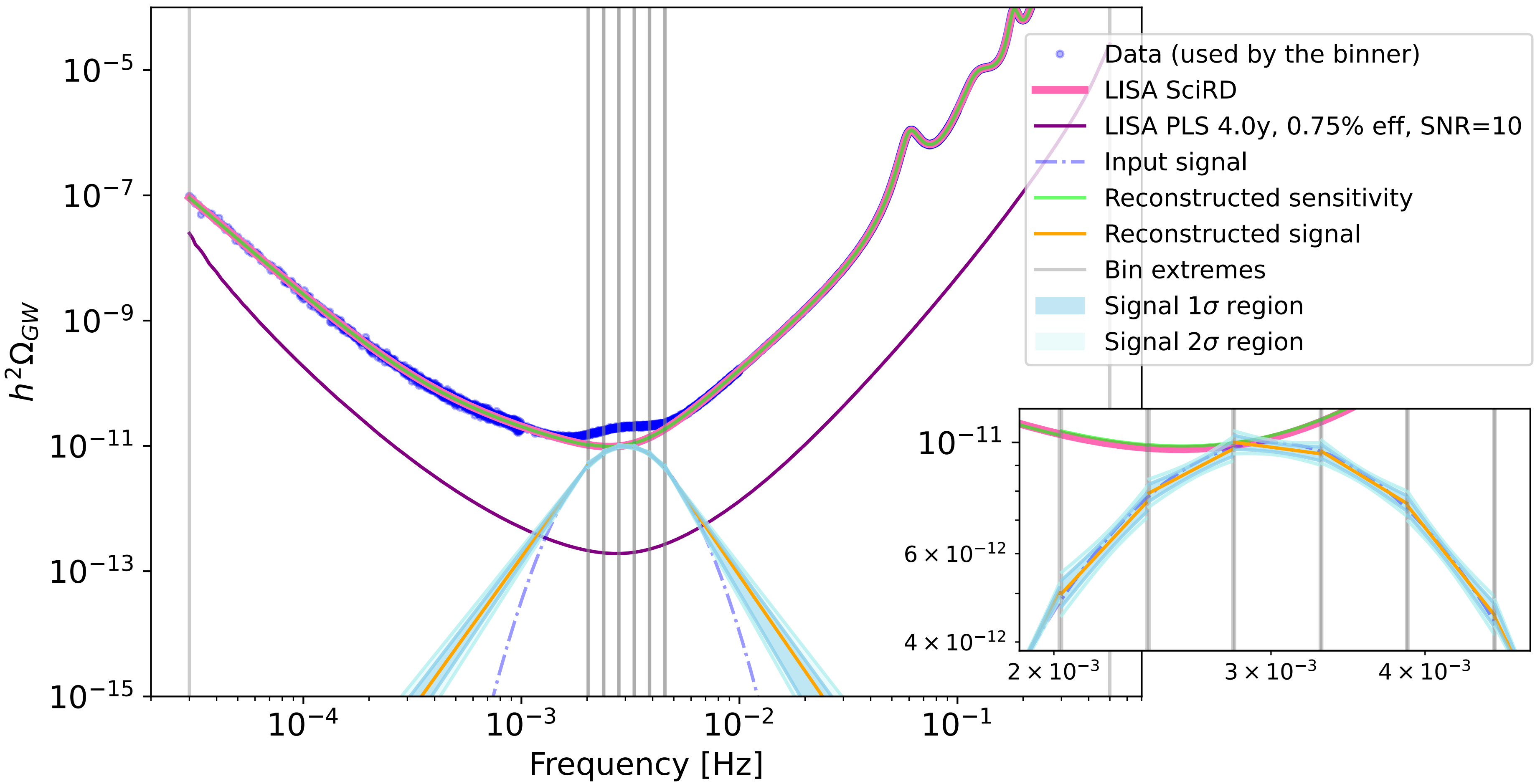

# Examples

Signal degenerate with XX noise auto-spectrum

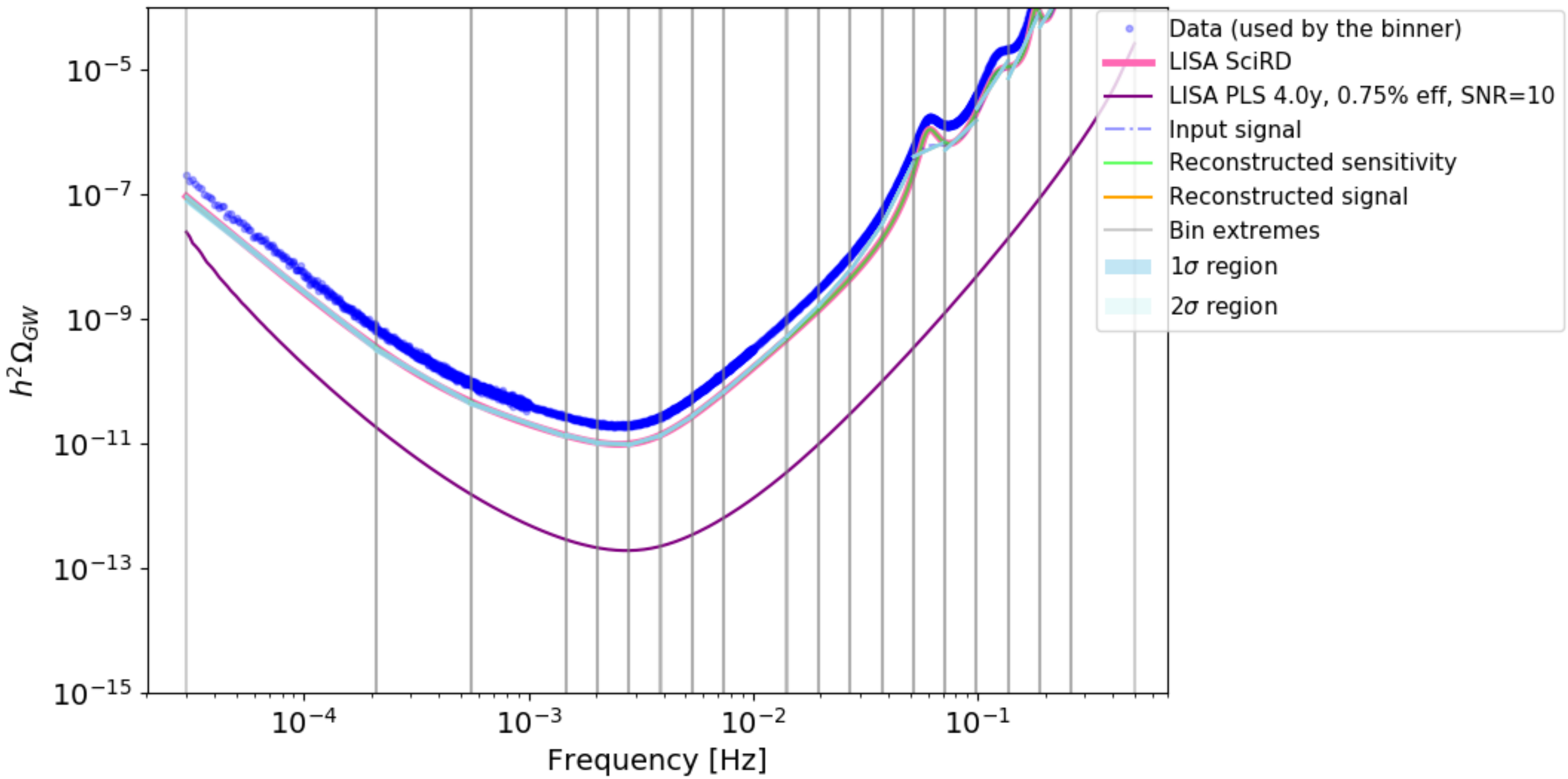


User of multiple channels allows to break degeneracies.

# Reconstruction with Foregrounds

Broken power law with galactic foregrounds

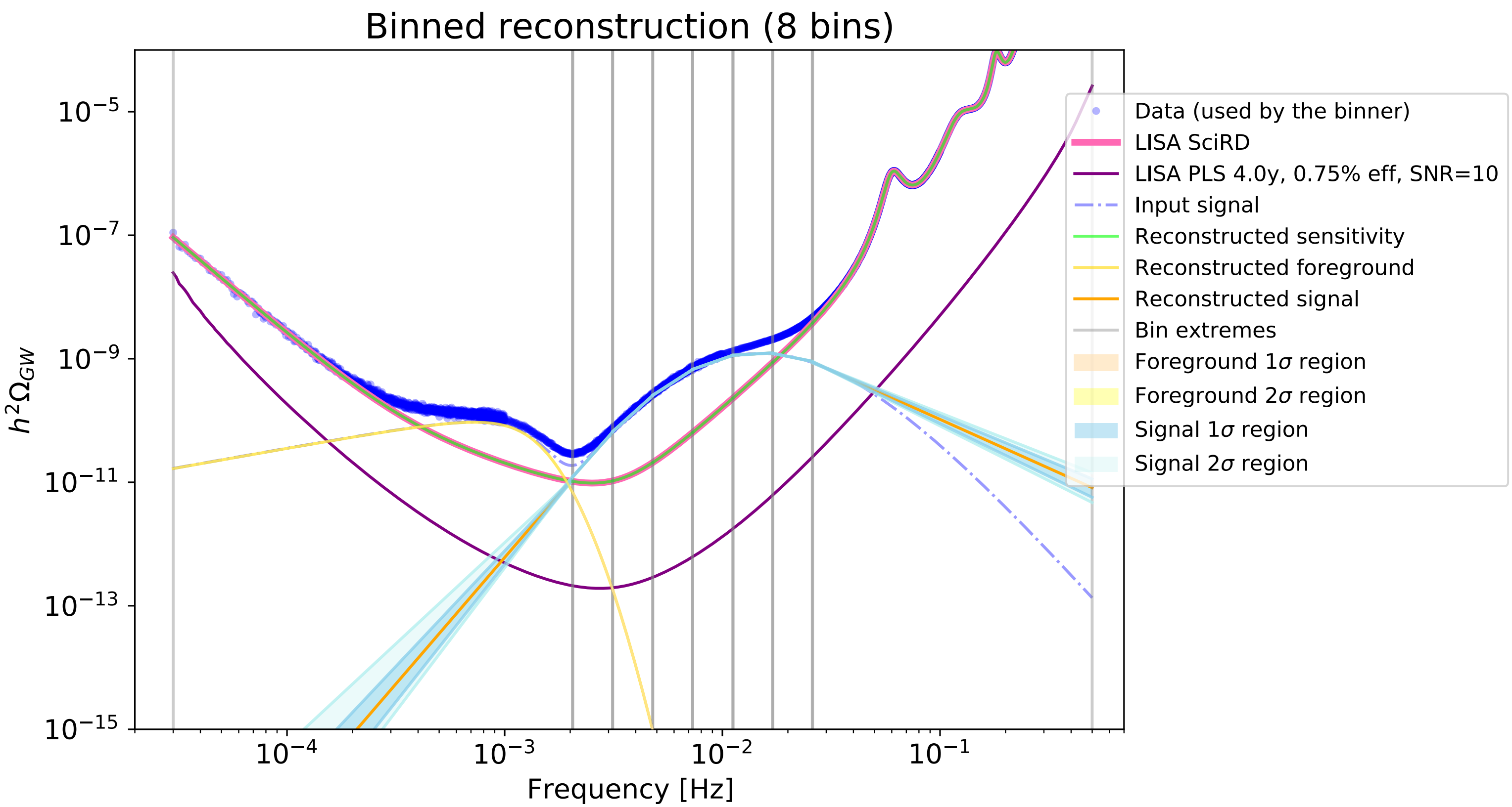


Good reconstructions is possible even in the presence of foregrounds.

# Conclusions

- There are many processes that could have taken place in the early universe that produce a stochastic gravitational wave background.
- LISA will be in a good position to constrain many of them.
- The shape is a priori unknown, motivating a model-independent search for a stochastic gravitational wave background.
- For a simplified setting, we have provided one such possibility, but improvements on several fronts are needed to confront real data.

# Thank you